

A Solar Electric Propulsion Cargo Vehicle to Support NASA Lunar Exploration Program IEPC-2005-320

Ronald Spores* and Jeff Monheiser†
Aerojet Corporation, Redmond WA 98073

Brian P. Dempsey‡, Darren Wade§ and Kenneth Creel**
Lockheed Martin, Denver CO 80201

David Jacobson††
NASA Glenn Research Center, Cleveland, OH 44135

Geoff Drummond‡‡
Colorado Power Electronics, Inc. Fort Collins CO 80524

In support of the President's 2004 Vision for U.S. Space Exploration, two NASA funded efforts were initiated for the development of critical propulsion technologies required for high-power solar electric propulsion (SEP) cargo vehicles. Results show that a high power SEP system is capable of delivering over twice the mass to the lunar surface as compared to a cryogenic chemical system. Since an SEP cargo system can be reused for multiple missions, this technology has the potential to save billions of US dollars in reduced launch cost. This paper mainly describes the effort on the High-Thrust Hall-Thruster program (HT)², which encompasses the detailed design, build, and test of an engineering model system including four high power (multi-kilowatt) thrusters, propellant flow controllers, next generation power processing units, and an advanced thermal management. As a result of the efforts on the (HT)², a 97% power converter module has been demonstrated. The second program is entitled Direct Drive Demonstrator (D3) and is responsible for designing, building and testing a complete, end-to-end, sub-scale direct drive SEP system for high delta-V missions. Mission analysis is presented showing the significant advantages of using solar electric propulsion to haul non-time critical mass from low-earth orbit (LEO) to the lunar surface.

I. Introduction

In the President's Vision for U.S. Space Exploration, presented January 2004, a new initiative for the nation was established to send humans back to the moon and ultimately to Mars for a sustainable presence allowing exploration. As part of this effort NASA funded programs to investigate technologies that will help to economically transport large amounts of supplies from low Earth orbit to the Moon. High power solar electric propulsion (SEP) offers a compelling alternative to chemical systems for these non-time

* Manager of Programs, Exploration Systems, Aerojet General Corporation, Redmond, WA

† Engineering Specialist IV, Exploration Systems, Aerojet General Corporation, Redmond, WA

‡ Senior Staff Engineer, Lockheed Martin Space Exploration Systems, Denver, CO 80201

§ Systems Engineer, Lockheed Martin Space Exploration Systems, Denver CO 80201

** Mechanical Engineer, Senior, Lockheed Martin Space Exploration Systems, Denver CO 80201

†† Research Engineer, Electric Propulsion Branch, NASA Glenn Research Center, Cleveland, OH

‡‡ President, Colorado Power Electronics, Inc., Fort Collins, CO

critical cargo missions due to its much higher specific impulse. Two efforts were initiated for the development of critical electric propulsion (EP) technologies required for high power solar electric propulsion cargo vehicles. The first of these programs, referred to as the High Thrust Hall Thruster program (HT)², encompasses the detailed design, building, and testing of an engineering model system including four high power Hall thrusters, propellant flow controllers, next-generation power processing units, and an advanced thermal management system. The second program, detailed here to a much lesser extent, is referred to as the Direct Drive Demonstrator (D3) and its goal is to design, build and test a complete, end-to-end, sub-scale direct drive solar electric propulsion system.

The principal objectives of these Exploration efforts is to: 1) determine if a reusable SEP cargo tug at > 500kW is feasible within a decade, 2) determine if trip times of less than a year are realistic, 3) assess the global supply of xenon and krypton propellant, 4) establish if an SEP tug has advantages over a state of art chemical stage and 5) design an initial SEP vehicle layout to determine which components give the highest payoff for further research investment.

For the (HT)² effort, Aerojet Redmond is responsible for program management and systems engineering for the propulsion system. Lockheed Martin contributions include: mission analysis, vehicle design, innovative lightweight heat pipe/radiator design and plume impingement and interactions. NASA-GRC is funded via an Intramural Call for Proposals (ICP) award to design and develop a high power Hall thruster. Colorado Power Electronics, Inc. is leading the development of an efficient, resonant topology power converter design. Initial assessment determined that a power level of 600 kW is a good trade off between solar array size and mission trip time. A multi-string architecture is being recommended with four 150 kW modules, each with a thruster, propellant flow controller, and conventional power processing units (PPU), as well as a thermal management system. This modular system of multiple high-power component strings is considered easily scaleable to accommodate varying mission power levels. Hall thrusters were selected for this high power SEP system due to their high thrust/power ratio and their high level of technical maturity (TRL) for power levels greater than 50kW. Further, Hall thrusters offer operational simplicity and integration ease over ion engines or liquid metal magnetoplasmadynamic (MPD) thrusters.

The key technical challenges for the High Thrust Hall Thruster system are developing and validating:

- a high power Hall thruster (~150kW) to TRL 6;
- clustering these high power thrusters in close proximity without adverse thermal, plume interaction, life or cathode coupling effects
- a lightweight thermal system to transport waste heat from PPUs and thrusters to radiators
- a high efficiency power processing unit (PPU)
- conceptual vehicle design and mission analysis for a cargo vehicle capable of hauling more than a hundred metric tones of cargo from LEO to a low lunar orbit (LLO)
- Spacecraft/plume interaction analysis, in particular on the large high voltage solar arrays; high power thruster and plume EMI and RF interference

For the D3 program, Aerojet Redmond is also responsible for program management and systems engineering. Lockheed Martin provides insight into solar array design and power system requirements. SAIC will model the spacecraft operating environment, and study the interactions of the solar array with the plasma. NASA Marshall along with the U. of Alabama at Huntsville will select and design the protoflight plasma diagnostics. NASA GRC will support both solar array design and system level testing and provide test facilities. An important outcome of this effort is the design of the control methodologies to ensure transients during start-up, shutdown, deep throttling, and dynamic events are compatible with spacecraft power system and component design. This paper discusses pros and cons of using a high voltage solar array in a direct drive mode as compared to a conventional array and power processing unit.

The key technical challenges for the Direct Drive Demo system are developing and validating:

- Start up and stable operation of a thruster without independent ability to control voltage and current through a conventional converter
- Operation of a high voltage solar array (~300 volts) in a thruster plasma environment
- The following components need development from TRL 4 to 6: an advanced digital propellant feed sub-system, a direct drive Thruster Control Unit (TCU), and a Low Voltage Power Unit (LVPU)

Each of the major sub-systems that are critical for assembling a high power SEP cargo tug are discussed in the following sections and a status is given of the technology maturity.

II. Mission Analysis and Requirements

Solar electric propulsion (SEP) cargo delivery systems can transport substantially more mass than a chemical system for a given initial mass in low Earth orbit (IMLEO) at the expense of trip time and vehicle dry mass. To illustrate this, a detailed mission analysis was conducted which directly compares cargo delivered for an optimized chemical propulsion system and an optimized SEP system. For this study, a lunar surface cargo delivery mission which fits within the current concepts for the Lunar Exploration Vision was analyzed. It is assumed that all chemical stages use liquid oxygen-liquid hydrogen propulsion with a specific impulse of 450 seconds. Further, both systems use the same chemical technology and scaling factors for the descent/landing stage.

The starting assumptions for both the SEP and chemical baseline tug missions were that a shuttle derived cargo vehicle will be capable of delivering 70 metric tons to a 550 km altitude circular orbit inclined at 28.5° to the Earth's equator. This launch vehicle assumption was developed merely to give a point comparison of the two types of systems and direct scaling of the systems should retain comparative applicability. The tug mission end point is a lunar equatorial orbit having a circular altitude of 100 km.

The launch vehicle delivery orbit trades take into consideration two factors for a tug with such a large scale solar array. The first is the effect of the eclipse duration on the trajectory and the second is atmospheric drag which has a direct affect on orbit lifetime. First, because of the very high power levels being considered, it is not feasible for the SEP vehicle to operate at full power while in eclipse due to the prohibitive mass required for a power storage (battery) system. Because of the computation complexity associated with determining an optimal trajectory which includes eclipse effects, an initial numerical experiment was conducted in which the fully optimized analysis was compared to a continuous burn trajectory, ignoring eclipse effects. The results of this experiment are presented in Figure 1. Comparing the full force simulation of the blue orbit to the continuous thrusting trajectory of the green orbit reveals only a slight difference between the orbits provided a 90 percent duty cycle is used. It should be noted that there was a distinct difference between the two analyses in terms of orbit phasing but for this study those differences could be and were neglected.

Another critical factor affecting the feasibility of a large, high power SEP system is the effect of atmospheric drag on the minimum operating orbit and the orbital lifetime of the transfer vehicle. To determine the minimum permissible starting orbit, which maximizes the delivered payload of the launch vehicle, the industry standard is to maintain a thrust-to-drag ratio greater than 10. To determine this ratio,

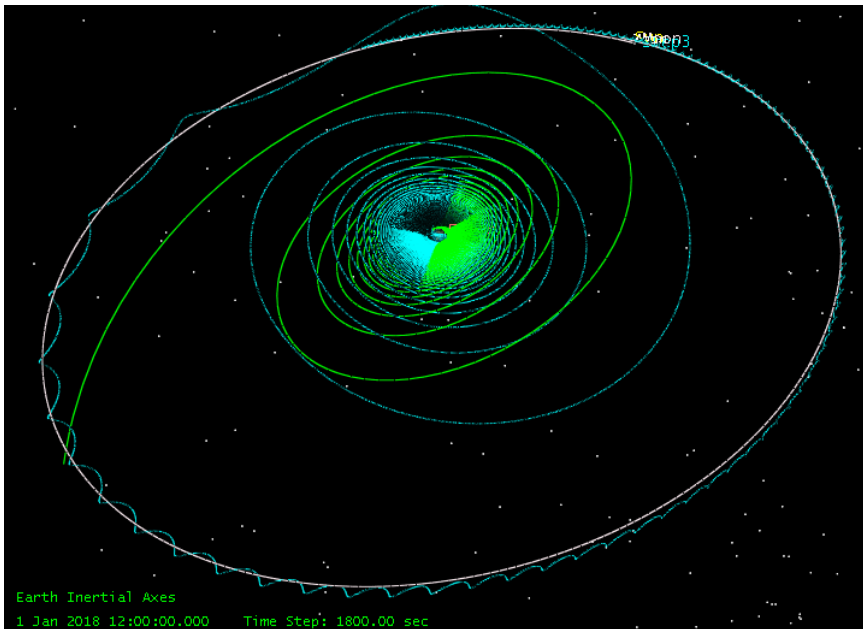


Figure 1 Eclipse (Non-Continuous Thrust) Simulated Trajectory (green oval) and Continuous Thrust (blue spiral)

the cross sectional drag area of a 600 kW array is assumed to be 2400 m^2 and a coefficient of drag, C_D , of 4 was assumed. The drag for the tug varies substantially throughout a low Earth orbit as the large solar array rotates from full ram to parallel with the velocity vector as the array tracks the Sun. This varying drag was handled by integrating the ram facing cross section throughout the orbit and generating an orbit-averaged cross sectional profile. Figure 2 shows that based on worst case solar max density results¹ and an I_{sp}

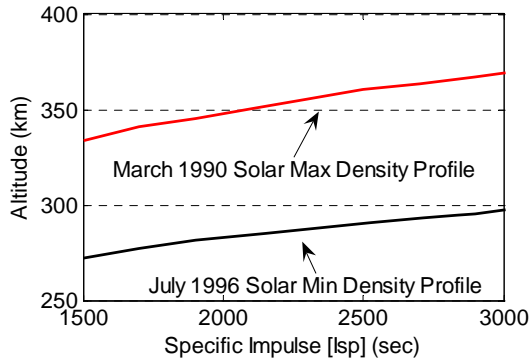


Figure 2 Minimum starting altitude for a 600kW SEP cargo tug with T/D=10.

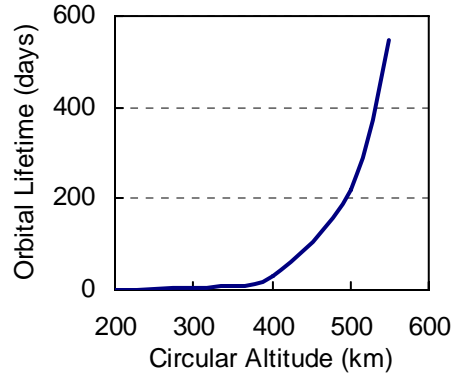


Figure 3 Orbital lifetime versus Altitude

=3000 sec, 375 km should be a safe minimal operating altitude. However, this does not take into account potential vehicle down times, i.e. if the vehicle goes into a ‘Sun Safe’ mode. Thus, orbital lifetime must also be taken into account. Assuming a 2018 launch, Figure 3 was generated using the STK/Orbit Lifetime tool along with a solar max case². At 550 km altitude the orbit lifetime is 1.5 years, which is deemed acceptable for ensuring the safety of the vehicle for extended parking durations; thus, 550 km was chosen as the launch vehicle delivery altitude for this study for both the chemical and electric propulsion tug concepts. For SEP vehicles returning to wait for the next payload, a 1000 km parking orbit was selected since it requires no drag make-up and requires less than 2 days to drop down to the launch vehicle delivery altitude.

The baseline chemical vehicle configuration is a single launch of a two stage spacecraft consisting of an orbit stage and a one-way descent/landing stage. The orbit stage performs both the Trans-Lunar Injection (TLI) and the Lunar Orbit Insertion (LOI). From 550 km circular Earth orbit to a 100 km circular lunar orbit, the total required delta-V for the orbit stage for a direct trajectory is 3050 m/s. For a 70 MT IMLEO, the vehicle requires 42.9 metric tons of propellant with an expended stage mass of 3.9 MT. From the 100 km LLO, the delta-V required for the descent/landing stage is 1894 m/s which corresponds to 8.1 MT of propellant required for landing on the lunar surface, leaving 15 MT of landed dry mass. Using scaling factors for landed vehicles, this landed mass results in 11.9 MT of delivered cargo to the surface of the Moon. The transit time for this complete mission is 4 days.

To investigate the potential advantages of an SEP cargo delivery system and explore vehicle design dependence, four configurations were considered along with two power levels and three different specific impulses to show the sensitivity to such parameters. In general, SEP cargo tug systems can deliver much larger payloads than chemical systems, however they require slow spiral transits out of the Earth’s gravity well and for this study also a Moon centric spiral transfer in towards the lunar surface. Three of the four configurations are reusable while the last vehicle demonstrates a one-way transit that stays in lunar orbit after deploying the descent/landing stage. The reusable variants consist of two separate vehicles, an orbital transfer vehicle (OTV) and a cargo delivery vehicle (CDV). All reusable components of the system, including the solar arrays, thrusters, PPUs are on the OTV. All components that are used only for the duration of the specific delivery mission including the cargo and propellant tanks are on the CDV. The OTV is the master in all docking operations and contains sufficient hydrazine propellant to dock with five separate CDVs. All electric propulsion trajectories were optimized with an internal Lockheed Martin code called ISOCS. The same delta-V requirements of 7830 m/s for the outbound leg and 7840 m/sec for the inbound leg were used for all SEP missions; an additional 500 m/s is allocated as margin. Table 1 summarizes the results of these studies and for configurations that require more than one CDV type, the first launched CDV is listed on the first line and subsequent launches are listed on the second line.

The first reusable configuration uses a separate evolved expendable launch vehicle (EELV) to deliver the OTV to its parking orbit, where the vehicle deploys its arrays and begins spacecraft checkout prior to launch of the CDV. This requires the OTV in this configuration to have the Hall effect thrusters as well as a small xenon propellant tank to perform checkout of the SEP system. This configuration has the benefit that there are only two vehicle designs and the operation of each lunar cargo delivery mission is identical.

A detriment is that this case requires an additional EELV launch and that even for the vehicle's first mission a space docking with its cargo is required. The OTV for this configuration, at a power level of 600 kW and an I_{sp} of 2500s, has an on-orbit mass of 8075 kg. Using the same scaling factors as the chemical system for the descent/landing stage, results in a landed stage mass of 26,975 kg of which 22,622 kg is delivered cargo. The transit time for this configuration is 6.6 months from LEO to LLO and another 1.3 months for the return to LEO. These results are listed as Configuration 1 in Table 1.

Configuration 2 has the OTV and CDV launching together on the same heavy lift launch vehicle. This allows the OTV checkout tank to be removed. This scheme reduces cost by eliminating the EELV launch and reduces risk by removing the docking requirement for the first mission. The penalty to the system is less delivered cargo mass on the first cargo mission and the need to develop two similar, but different sized CDVs. Cases were also run where both power and I_{sp} were varied from the baseline 600kW and 2500s.

Configuration 3 also uses configuration 2's combined OTV and CDV on one launcher strategy, but addresses the potential concerns of low pressure fluid connectors between the OTV and CDV by moving the hall thrusters and all propellant management devices to the CDV. Unfortunately, this scheme now requires a high-voltage high-power connector between the PPUs on the OTV to the thrusters on the CDV. The benefit is that all fluid connectors between vehicles has been removed, however the cost to the system is the replacement of the hall thrusters and propellant management devices for each mission along with the reduced cargo capability for subsequent launches as compared to Configuration 2.

Finally, a disposable configuration was generated to illustrate the minimal cost to the reusable systems for returning to LEO. As such, all components related to docking the OTV with the CDV have been removed. The OTV assumes the entire role of the CDV in this configuration including carrying the descent/landing stage. As can be seen in Table 1, the increase in delivered cargo to the surface for configuration 4 is minimal, showing that the cost of returning the OTV to LEO is negligible to the system.

Table 1 Comparison of Cargo Delivery Configurations

Configuration	Power Level (kW)	I_{sp} (s)	OTV On-Orbit Mass (kg)	CDV dry mass without descent/landing stage (kg)	Surface Cargo Delivered (kg)	LEO-LLO Transit Time (mo)	LLO-LEO Transit (mo)	Xenon Prop Mass (kg)	Thruster Life Consumed (hrs)
Reference Chemical	N/A	450	N/A	N/A	11,900	0.13	N/A	N/A	N/A
1	600	2500	8075	2338	22,622	6.6	1.3	25,502	5686
2 (first CDV follow on CDV)	600	2500	7996	1840 2120	19,690 22,439	5.9 6.5	1.2 1.2	23,001 25,553	5128 5698
2 (first CDV follow on CDV)	600	3000	7996	1770 2060	21,549 24,830	7.2 8.1	1.5 1.6	19,548 21,619	6276 6941
2 (first CDV follow on CDV)	600	3500	7996	1770 1993	23,071 26,518	8.6 9.6	1.7 1.8	16,952 18,735	7409 8188
2 (first CDV follow on CDV)	450	2500	6465	1770 2060	20,735 23,080	7.8 8.6	1.4 1.5	22,498 24,512	6689 7287
3 (first CDV follow on CDV)	600	2500	6880	2810 3093	19,377 22,085	5.9 6.5	1.2 1.3	23,146 24,570	5161 5616
4	600	2500	7400	N/A	23,210	5.8	N/A	18,990	4234

III. Conceptual Layout of Cargo Transport Vehicle

The design of a large SEP space vehicle presents several unique challenges. Almost all spacecraft have at least two configurations; the stowed configuration, which must fit within a launch vehicle payload fairing, and one or more deployed configurations for mission operations. In order to demonstrate that it is

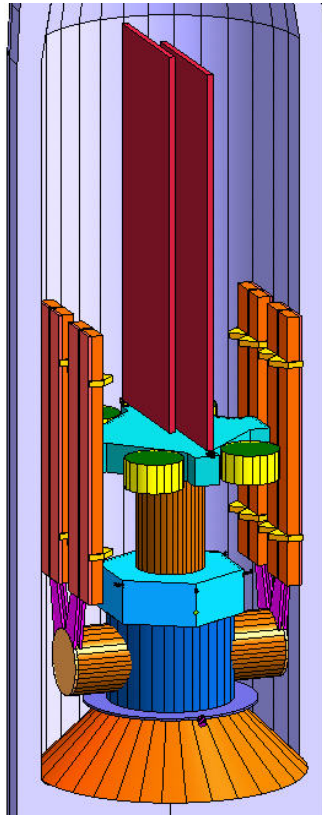


Figure 4 Vehicle stowed within standard 5m Atlas payload fairing

possible to design, build and launch a 600kW SEP vehicle, standard Atlas V launch vehicle constraints were placed on the design including the envelope for a standard 5 m payload fairing. This was done to illustrate that such a tug is feasible even without the substantial investment in a new heavy launch vehicle. For an SEP cargo tug, the principle feature that presents a stowage problem is the exceptional large solar arrays. In order to show that the stowage issue is solvable, a conservative approach was taken here to use a scaled up version of the flight proven solar array configuration built by Lockheed Martin for the International Space Station (ISS). This hardware is at TRL 9 and thus already been proven that it can be compactly stowed and deployed in the space environment. A 600 kW solar array using multi-junction GaAs would require about 2,600m² of collection surface. This could be accomplished by using the Space Radar Topography Mission boom to deploy ISS type solar array wings that are 60m long. The 22m wide (HT)² wings are deployed on each side of the transfer vehicle and capable of one axis pointing. These solar array wings are retractable which may be advantageous during docking. Multiple, advanced solar array technologies are discussed in section VI, each having its own advantages. These technologies will allow for an even further reduction in the

stowage volume over the coming years. Figure 4 show how the arrays and radiators are stowed while Figure 5 shows the deployed configuration for a 600kW vehicle.

The Hall thrusters while large, do not present any special problem for this spacecraft from a design standpoint. Another nonstandard spacecraft feature on this vehicle is the docking mechanism. The docking mechanism is modeled from the design of the Johnson Spaceflight Center low impact docking system (LIDS) docking mechanism. In addition to providing the mechanical connection between the cargo and transfer vehicles, it also provides propellant transfer, electrical power and data connections. The propellant transfer connection is simplified because of the decision to store the xenon cryogenically at low pressure thus the transfer connection need only be capable of handling 1.7MPa (250 psi). The final nonstandard features for this spacecraft are the large radiators necessary to remove waste heat from the PPU's. The radiators are 6.5 m x 2.3 m each and require a yet to be determined circulating fluid to remove approximately 24kW of waste heat. Remaining spacecraft subsystems are off-the-shelf equipment with long heritage of space flight and are placed inside the bus module in a standard configuration.

The cargo carrying vehicle is designed to be as simple as possible and is assumed to be launched by a 70 MT launch vehicle with no special requirement on the payload fairing envelope. The largest single component of the cargo vehicle is the low pressure (1.7 MPa) cryogenic liquid xenon tanks. The tanks are maintained at a temperature less than -35C via passive shading from the sun, and by using high emissivity optical coatings. This configuration saves substantial weight over large high pressure tanks, see section IX. The cargo vehicle is also assumed to carry a chemically propelled lunar lander which has been defined by the Lockheed Martin CE&R architecture study³. Cost, mass, risk and performance metrics do not indicate that there is one design that is clearly better than all others. Once clear vehicle requirements are available, trade studies will have to be performed using these other metrics.

Once the stowed and deployed configurations are defined for both vehicles and all the requirements for the necessary subsystems are established, a master equipment list (MEL) can be created. The MEL serves several purposes; the most important being to break down the various subsystems into components so that

an overall vehicle mass can be estimated. Later the MEL is used to derive electrical power, data, and cost estimates. When the hardware in question is off-the-shelf with flight heritage, a mass margin of 6% is assigned to cover minor redesigns or custom fittings which may become necessary to integrate the part. When the hardware is new or developmental in nature, a margin as large as 40% is used to cover mass growth during development. The preliminary MELs for the transfer vehicle is shown in Table 2. The MEL for the transfer vehicle shows that this vehicle is well under the maximum mass payload (20,000kg) of the Atlas 531 heavy launch vehicle. For mission analysis purposes the conservative mass with margin is used.

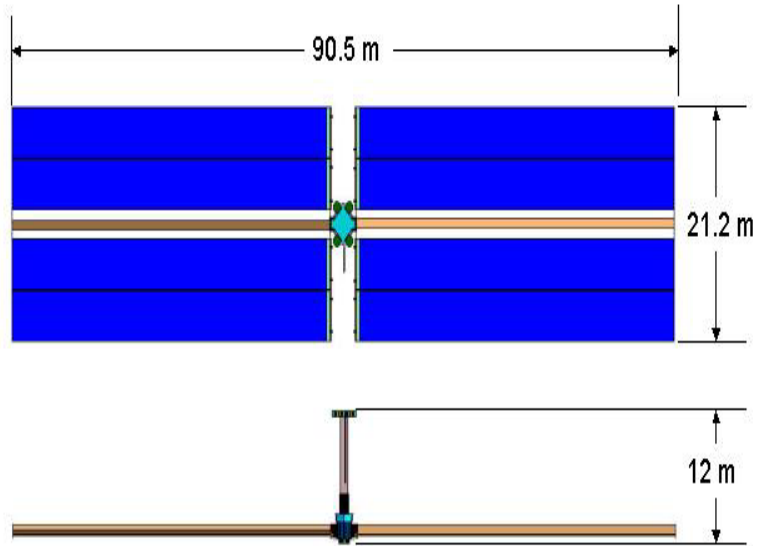


Figure 5 Final On-Orbit Space Vehicle Configuration

Table 2 Projected (HT)² Masses

Nomenclature	Total Estimated Mass (Kg)	Contingency (%)	Total Estimated Mass w/Contingency (Kg)
Telecom	11	8%	12
EPS	3,510	25%	4,388
GN&C	106	5%	112
Structure	770	20%	924
Thermal	192	20%	230
Mechanisms	557	20%	669
ACS Propulsion	62	8%	67
Hall Thruster System	1,110	15%	1,277
Ballast	10	0%	10
Expendables	370	5%	389
(HT)² Cargo Vehicle	6,698		8,076

IV. High-Power Hall Thruster Design

Of the available electric propulsion systems, Hall thruster technology is particularly well suited for the application of an SEP cargo tug. This is principally attributed to higher thrust for a given power level that is characteristic of Hall thrusters, see Figure 6. Cargo delivery applications are expected to require moderate trip times; at the most being a year for a round trip. This constraint corresponds to an optimum specific impulse between 2500-3500 seconds, depending on the spacecraft power level; state-of-the-art Hall thrusters operate efficiently over this range. Hall thruster systems also offer system benefits over an ion thruster system due to the lower mass and volume; they offer an advantage over magnetoplasmadynamic (MPD) thrusters due to maturity and thus lower level of risk.

The system power levels for these heavy cargo delivery applications are generally greater than 500 kW, depending on the destination, required trip time and particular mission scenario. These system power levels require that the single unit thruster power level be greater than 100 kW to minimize system

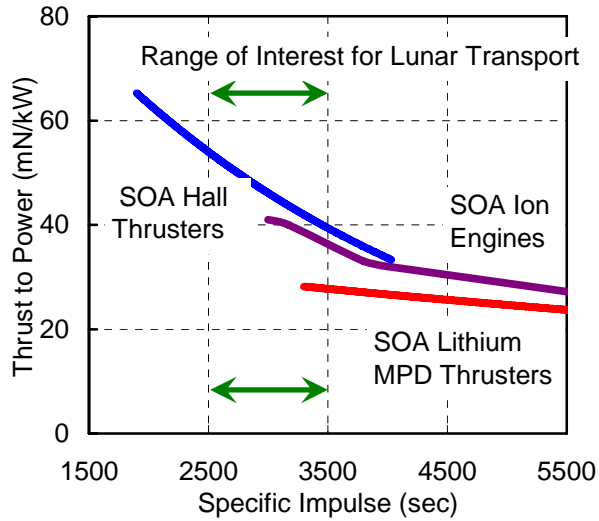


Figure 6 Comparison of T/P for Several EP Technologies

impulse of 2500 seconds at the 50 kW design point.⁵ During subsequent investigations the thruster was operated above its design power density up to 95 kW. The design and evaluation of the NASA-457M raised 50 kW class Hall thruster technology to a TRL 3 and reduced the technical risk of developing higher power Hall thrusters. NASA GRC initiated the design of a 150 kW Hall thruster operating at a nominal discharge voltage of 600 Volts and a discharge current of 250 Amperes. The predicted performance is shown in Figure 7 along with the measured performance of existing NASA Hall thrusters.

During the initial design phase, three discharge channel configurations were evaluated on the basis of thruster magnetic circuit mass, thruster footprint area, and channel width for a given channel area. The discharge channel geometries considered included: 1) a traditional annular channel, 2) high-aspect ratio (two semicircular sections connected by two straight sections) and 3) nested configurations (multiple circular discharge channels within a single thruster unit). Using the same power density as previously demonstrated NASA Hall thrusters, the thruster area for the nested configuration is 50% less than the traditional annular channel configuration while the high-aspect ratio configuration was 34% less. To determine if a non-conventional thruster configuration offers a reduction in mass in addition to footprint area, a magnetic circuit was designed for the traditional annular and nested configurations; see Figure 8. Both designs used the same channel width, depth and magnetic field characteristics. The magnetic circuit mass of the nested configuration was approximately 25% less than the mass of an equivalent circuit in a traditional annular configuration.

Despite findings that non-conventional discharge channel configurations offered both thruster mass and footprint area benefits, a traditional annular configuration was selected for the final design; this selection was made due to higher TRL and corresponding lower risk for the traditional design. The final discharge channel dimensions for the NASA-1000M Hall thruster were selected using the current density of state-of-the-art Hall thrusters and a magnetic circuit with a 1 meter outer diameter discharge channel was designed. Using a commercially available, three-dimensional magneto-static computer code the magnetic circuit was optimized and a plasma lens magnetic field line topography

complexity and improve reliability relative to using a much larger number of lower power thrusters. However, a significant gap in power level exists between existing technology and 100 kW class Hall thrusters. At the present time, 1.35 kW Hall thrusters developed in Russia are commercially available and qualified for use on Western spacecraft and the 4.5 kW BPT-4000, which operates up to 1,900 seconds specific impulse is nearly flight qualified.⁴

To address the need for higher power, moderate specific impulse Hall thruster technology, NASA Glenn Research Center (GRC) has designed and evaluated the performance of devices with these characteristics. The NASA-457M, was designed and operated with a discharge specific

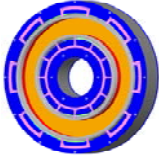
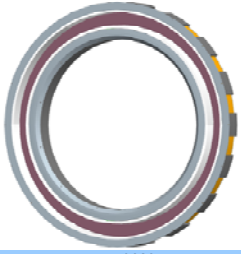
Thruster	NASA-173M	NASA-457M	NASA-1000M
			
Power	8 kW	50 kW	150 kW
Thrust	0.35 N	2.45 N	6.5 N
Isp	2800 S	2500 S	2900 S
Lifetime	6,000 hrs	8,000 hrs	30,000 hrs
Efficiency	0.60	0.60	0.65

Figure 7 The performance characteristics of NASA Hall thrusters

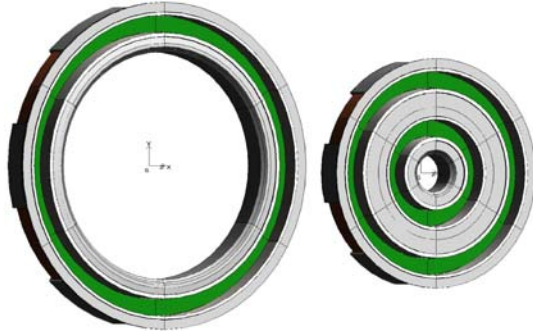


Figure 8 The traditional annular and nested Hall thruster configurations

was achieved.⁶ The mass of the 150 kW thruster's magnetic circuit including the magnetic iron and electromagnet components was 136 kg; this compares favorably with a linear scaling of the magnetic circuit mass of lower power Hall thrusters. A three-dimensional solid model of the NASA-1000M has been generated and mechanical and thermal analysis will be completed as part of the thruster design.

High-current hollow cathodes necessary for experimental testing of NASA's 50 kW Hall thrusters have been developed.⁷ However, the 100 Ampere emission current provided by existing hollow cathodes is insufficient for the

150 kW Hall thruster project. Therefore, a laboratory model hollow cathode was designed with emission current and lifetime parameters that are consistent with the NASA-1000M Hall thruster. An emitter has been designed to provide 250 Amperes emission current while maintaining a current density and temperature consistent with flight qualified hollow cathodes, which have demonstrated lifetimes of 30,000 hours^{8,9}. While similar lifetimes are expected for the 250 Ampere cathode, the use of multiple hollow cathode assemblies, to facilitate the reusability of cargo delivery vehicle, is also considered to be feasible.

To maximize the economic benefit of SEP cargo delivery, the number of trips from LEO to the desired destination needs to be maximized. Mission analysis performed for a Lunar cargo delivery mission indicated 5 trips from LEO to low lunar orbit was possible, which corresponded to required Hall thruster lifetimes up to 50,000 hours. This requirement significantly exceeds the lifetime of state-of-the-art Hall thrusters, which is approximately 6,000 hours¹⁰. As part of the 150 kW Hall thruster project, NASA GRC is also implementing an approach to significantly increase the lifetime of Hall thrusters. This approach eliminates discharge channel erosion as the life limiting mechanism through in-situ renewal of the ceramic discharge channel. This will be accomplished by mechanically advancing the ceramic discharge channel walls as the downstream edge erodes due to interaction with the plasma. The actuation requirements have been defined and a conceptual mechanical design was completed for a sub-scale power Hall thruster; testing is scheduled for next year.

V. Power Processing and Control for High Power Hall Thruster Systems

The present state of the art for power conversion technologies used within the Power Processing Units (PPUs) of electric propulsion system utilize a "soft switching", switch mode topology. By leveraging successes within the semiconductor processing industry, this program is advancing the SOA by evolving a full resonance topology to the aerospace industry. In contrast to the square waveforms used in a switch mode power converter, a full resonant topology adds both inductance and capacitance to the input of the converter to create a sinusoidal waveform for the power conversion. The values of the inductive and capacitive circuit components are chosen such that they establish a resonance condition at the switching frequency, i.e. $f_s = \frac{1}{2\pi\sqrt{LC}}$ where f_s is the resonant frequency, and LC is the product of the circuit inductance and capacitance.

The ability to create sinusoidal waveforms eliminates the high frequency harmonics associated with square waves, giving the full resonant topology the ability to operate at much higher switching frequencies which leads to a significant reduction in the power magnetics mass. A full resonant converter approach virtually eliminates the high voltage spikes across the output diodes and allows much smaller output filters to be used making the design more reliable, efficient and cost effective.

To demonstrate the advantages of a full resonant power converter, Aerojet and Colorado Power Electronics designed, constructed, and tested a prototype 1 kW converter. Compared to standard semiconductor industry resonant converters, this design paid particular attention to minimizing the losses within the power conversion circuits in an attempt to achieve the highest possible conversion efficiency. Figure 9 shows a plot of the power conversion efficiency as a function of the output power for a constant input voltage of 150 V DC and two different output voltages, 400 V DC (circles) and 750 V (squares). The conversion efficiency data presented here show the values obtained both excluding (solid symbols) and

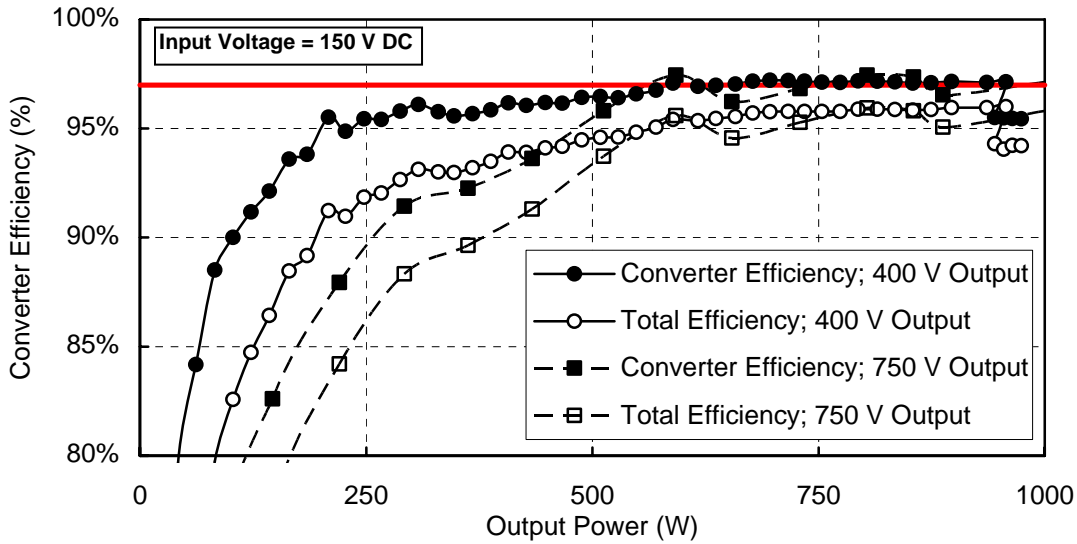


Figure 9 Performance measurements on a 1 kW full resonant converter show extremely high efficiency (97%) over a 2:1 throttling range from the full power output of 1 kW down to 500 W.

including (open symbols) the auxiliary power components. For this prototype design the majority of the auxiliary power was used to power the gate drive circuits which were not optimized, therefore with further improvements the auxiliary power can be reduced in future designs. The conversion efficiency of this power converter is near or greater than 97%, the red line, over the power range from 500 W to 1 kW which is the highest conversion efficiency of any converter produced by Aerojet. Having an extremely high efficiency over a 2:1 output power and voltage range is an important feat with significant implications for solar electric propulsion missions where the output power of the solar array diminishes throughout the mission.

A. Discharge Converter Sizing

Once a preferred converter topology had been determined, the optimal power level needs to be specified. The main parameter that is analyzed for the electric propulsion system was the mass of the entire power processing unit. To do this, two different power system architectures were investigated; the first (Figure 10a) scheme is where the PPU's provide power to a common system power bus onto which the individual Hall thrusters are attached (left side of figure). This system has several advantages:

- The power level of each PPU and Hall Thruster can be optimized independently of each other.
- The propulsion system is flexible in that individual power processing units or thrusters

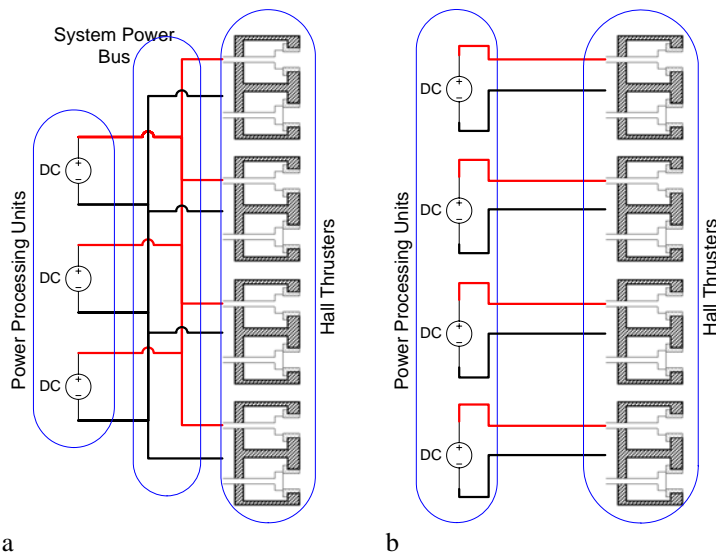


Figure 10 Two possible system architectures for operating multiple Hall thrusters either off of a common system bus (a) or from individual power processing units (b).

could be removed or added to the bus in the event of a single point failure.

The disadvantages are:

- The impedance of each Hall thruster must be exactly matched or a single thruster could consume a disproportionate share of the total power which could significantly affect the system performance.
- System integration is more complex since the number of discharge converters is determined by their optimal power level while the heater, keeper, magnet, and flow control system would be determined by the number of engines.

The second system architecture is a more conventional design in that the maximum power level of each PPU would be limited to the power level of the individual thruster. The advantages are:

- simple to integrate into the spacecraft since each PPU and thruster pair is a single unit.
- no power sharing problems between the individual thrusters

The disadvantages are:

- individual PPUs and Hall thrusters would be optimized for their operating power not the total system power; this option will likely have a mass penalty since lower power systems tend to have higher specific masses.
- The system is more susceptible to single point failures since it can not be easily reconfigured to accommodate single faults within different PPU/thruster systems.

Based upon these two system architectures and historical specific mass information (

Figure 11), the masses of a 600 kWe power system were computed first assuming a maximum output power level of 600 kWe and then second assuming a 150 kWe power level (the maximum for a single thruster). Performing these calculations using the empirical curve fit of

Figure 11 yields a mass of 420 kg for the single 600 kWe PPU and 153 kg for a 150 kWe PPU or 612 kg for the system of 4 PPUs. This clearly indicates that from a single unit mass perspective, it is better to build large PPUs at high power levels. However, if an N+1 redundancy requirement is imposed on the system then there exists an optimal power level since it is inefficient to carry an entire extra 600 kWe PPU for redundancy. Presented in Figure 12 are the total masses of the power processing system as a function of power level for the two cases where the entire system power can be provided by a single PPU, i.e. the system power bus architecture (solid curve) and the case where the PPU power has an upper limit equal to the maximum thruster input power (150 kWe), i.e. the individual thruster/PPU combination, the dashed curve. It should be noted that in computing the system mass, estimates for the dashed curve, the mass of an individual thruster/PPU was multiplied by four to account for the total number of individual thrusters in the system. These curves show that as the PPU output power increases there is a local minimum in the system mass

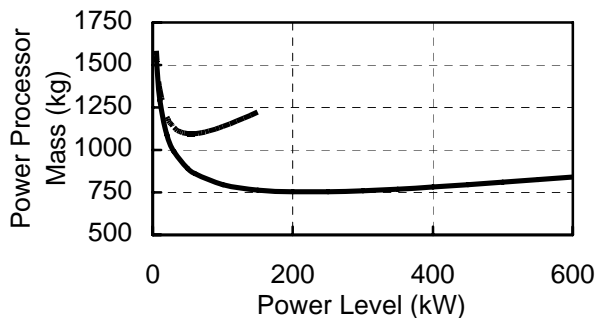


Figure 12 Projected Masses for the two different PPU architectures under study.

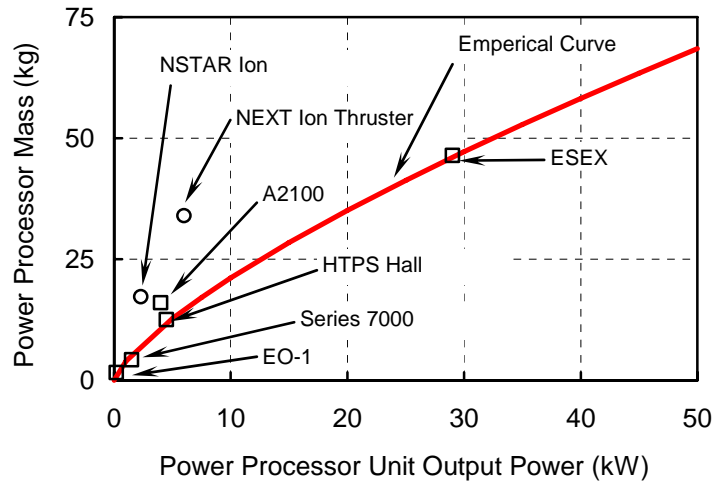


Figure 11 Power processor masses for various electric propulsion thrusters as a function of their total output power.

around the 200 to 250 kWe power level. This suggests that for the architecture of Figure 10a, the minimum system mass will be achieved by using four (three plus one redundant) 200 kWe PPUs. However for the individual thruster optimized system (Figure 10b), the optimal power level is about 50 kWe which suggests that each thruster should be powered by four (three plus one redundant) 50 kWe PPUs. Figure 12 indicates that the system mass for the individual thruster/PPU architecture is about 350 kg more massive than the common bus system.

Ultimately it was decided that the most versatile system would utilize 50 kW converters designed to be operated in parallel despite the higher system mass of this approach. At the present phase of this development program, however, it was felt that the development of a single 50 kWe converter was too large of a technical leap so it was decided to take an intermediate step of designing and building a 10 kWe converter which can be used to further develop higher power versions. Some of the technical challenges of designing a 50 kWe converter are in the power magnetics, very large eddy currents within the layers of the boards causing parasitic inductance problems, and concern about the availability of the high power switches required for the switching circuits.

B. Direct Drive Thruster Control

Present Hall thruster systems use conventional power processing units in combination with standard solar arrays operating from 28 V to 120 V. For power levels less than about 50 kWe these systems are ideal and the use of a PPU brings many benefits to a Hall thruster system, such as:

- isolation of the thrusters system from the spacecraft power bus and solar arrays
- control of the thruster discharge current and voltage which are directly related to the thrust and I_{sp}
- the ability to operate over a wide input voltage range associated with traditional arrays.

However, for future high power (hundreds of kilowatt to megawatt) systems the present output voltage levels associated with today's solar arrays require unacceptable current levels leading to excessive cable masses as well as high I^2R losses within the cabling. To minimize these disadvantages, several researchers^{11,12,13} have investigated the option of creating high voltage solar arrays, operating at voltages above 300 V, and directly connecting them to the input of the Hall thruster. This configuration has been termed "direct drive" and its use can lead to a significant reduction in PPU system mass by eliminating the costly and massive high power converters. This increases the overall PPU efficiency and reduces waste heat, thereby reducing the size and mass of the spacecraft thermal radiator system.

In a direct drive system, the traditional power processing unit is removed and replaced with two new components. The first is a Low-Voltage Power Unit (LVPU), and the second is a Thruster Control Unit (TCU). The LVPU is used to down convert the high voltage from the solar array bus to a voltage level more typical of existing spacecraft buses. This allows existing spacecraft components such as star trackers, on-board computers, etc., to be used without having to be re-designed and re-qualified for the higher input voltage. The function of the TCU is very similar to a conventional PPU in that it is used to interface with the on-board spacecraft computer, process commands associated with the thruster by controlling the propellant flow, the cathode heater and keeper as well as the thruster magnets. The TCU is also responsible for acquiring and processing the telemetry data along with performing basic health monitoring to ensure proper operation of the Hall thruster system.

Previous programs have demonstrated^{11,12} the feasibility of a direct drive system by showing that a Hall thruster can operate stably when connected directly to a high voltage array. Presented in Figure 13 are data that were obtained during a recent direct drive demonstration test. It should be noted that for financial reasons the program performing the test of Figure 13 could not afford a complete 4.5 kWe array so a programmable power supply was used to simulate the IV characteristics of an array. As can be seen in the figure, the operating points of the Hall thruster were compatible with the characteristics of the array. In these tests the start-up characteristics of a Hall thruster were assessed to make sure that the initial in-rush current did not exceed that which could be supplied by the array.

There are still some concerns that the start-up and transient characteristics of a Hall thruster are not fully compatible with the IV characteristics of a solar array. A new program was funded by NASA to build on the experience gained to date and further the understanding of the interaction between a Hall thruster and a solar array. Recent efforts have shown first order feasibility of the direct drive concept with evaluations of high voltage solar arrays and direct drive system characteristics. However, ground test simulation of the space environment relevant for plasma interaction is limited and this technology demonstration mission will provide critical input to the engineering of high power (>500 kW) EP systems.

VI. Solar Array Technologies

A 600 kW solar array for spacecraft application is a significant challenge since the largest solar arrays to date are the International Space Station (ISS) solar arrays with a planned total power capability of 110kW¹⁴; See Figure 14. Solar cell vendors have been increasing the efficiency output of multi-junction crystalline solar cells to greater than 28%¹⁵ commercially and greater than 35%¹⁶ in laboratory units and thin film solar cells to >13%¹⁷ commercially and greater than 19%¹⁷ in the laboratory. Air Force Research Laboratories

(AFRL) in Kirtland, NM is developing photovoltaic technologies to support the PowerSail program, which plans to fly solar arrays with 50 to 100kW power generation capability¹⁸. The Power Sail effort is developing light weight solar array structures for large deployed arrays with low packaging volume. Flight solar arrays of 1MW are being developed for use on the High Altitude Airship (HAA) by Lockheed Martin Space Systems. Fortunately, the technologies developed by ISS, HAA, solar cell vendors, NASA, NREL, and AFRL provide multiple options to achieving a 600kW spacecraft solar array.

Multijunction GaAs based solar cells are typically 5.5 mils thick. Work performed by Sharp¹⁹ and others looks at reducing the solar cell thickness to below 1 mil. The thinned multi-junction GaAs cells provide both the benefit of high power density (W/m^2) due to their high efficiency and high specific power (W/kg) due to the lower mass of the cells. These improvements translate into reduced solar array area and mass. The cell mass is reduced when multi-junction cells are lifted off the standard Germanium substrate and then supported on a lighter substrate or perhaps on the back of the cover glass. While these cells may have improved radiation tolerance, they would still require a thick cover glass for protection.

Significant advances have been made in Amorphous Silicon and Copper-Indium-Gallium-Diselenide (CIGS) thin film solar cells that are being laid down on flexible thin metal and polymeric substrates. NREL has developed CIGS cells that have >19%¹⁷ efficiency at the coupon level. CIGS manufacturers are making rapid progress to increase the production level efficiencies at low cost compared to multi-junction cells. These cells are radiation tolerant, low cost and have very high specific power even though the cell efficiencies are lower than multi-junction solar cells.

Since an SEP cargo delivery system (CDS) transits slowly through the Van Allen belts, the solar arrays would receive a high radiation dose. The radiation is largely due to proton fluence; both multi-junction and thin film solar cells are much more susceptible to proton fluence than electron fluence. For one study, an electric CDS is assumed to go through this high radiation environment for 6 outbound and 5 return trips. In this case, GaAs cells would require at least 12 to 20 mils of cover glass, adding significant mass, to reduce radiation induced degradation. CIGS cells degrade significantly in a high proton fluence but damage is annealed out at the operating temperature of about 70°C²⁰. The result is that the cells maintain about 80% of their original output

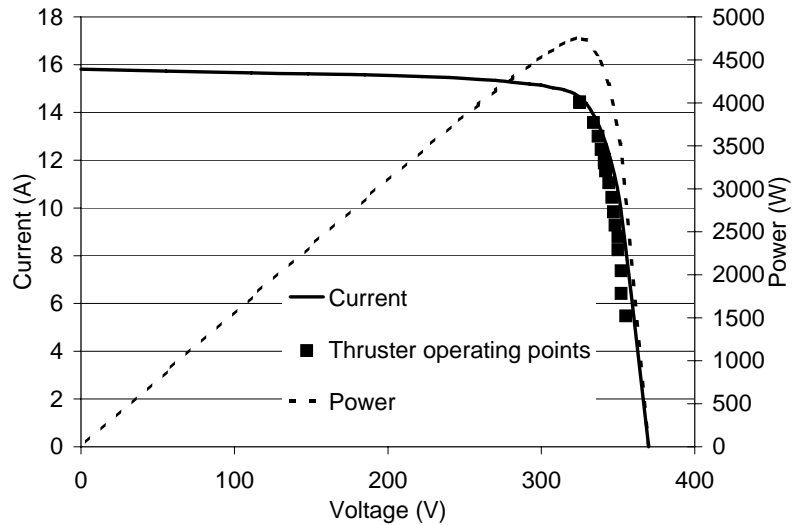


Figure 13 Thruster current and voltage levels demonstrated during Direct Drive operation.



Figure 14 ISS solar array being tested at LMSS, Sunnyvale

power without added cover glass protection. MDS-1 tested terrestrial solar cells in the laboratory and in the Van Allen Belts. The results of these tests showed that terrestrial CIGS thin film cells had almost no degradation in space and terrestrial GaAs multi-junction cells exhibited “sufficient” radiation tolerance.²¹

An Able-Entech refractive concentrator array called the Stretched Lens Array (SLA) solar array was also investigated.²² The approximately 8 to 1 concentrator uses high efficiency multi-junction GaAs cells and increases the efficiency of the cells slightly. The concentration allows the use of reduced solar cell and cover glass mass although the concentrator and heat rejection of the magnified cells adds mass back to the solar array module. This allows the cover glass thickness to be increased with a lower mass penalty than with non-concentrator arrays. The thicker cover glass and additional protection that form the concentrator lens provide increased radiation protection to the solar cells. The stowed packaging density has improved significantly with the latest flexible concentrator technology but still requires accurate sun pointing of within several degrees, on the alpha axis. Entech recently studied the robustness of the SLA technology to radiation degradation, and showed via analysis that it could withstand 13 slow spiral transits of the Earth’s Van Allen belts (7 outbound and 6 return trips).²³

Another concentrator that would offer high radiation tolerance for this application is the Survivable Low Aperture Troughs (SLATS). This solar array concentrator was baselined on the AFRL Survivable Power System (SUPER) program because of its high radiation tolerance. The use of high efficiency multi-junction solar cells and higher concentrations would make this technology competitive, although it may be heavier and have a lower stowage density than other technologies.

To calculate a solar cell module power density, the mass due to the cover glass or coating for thin films, inter-connect wiring, bypass diodes, blocking diodes, adhesives and mounting substrate must be summed. Conventional rigid panel substrates would be impractical for a solar array at the 600kW power level from a mass and stowage volume consideration.

Three solar array technologies currently appear feasible for creating a 600kW array. The thinned multi-junction GaAs cells provide high efficiency and would require a 2,600m² array, but the thick cover glass and back side radiation protection increases the specific mass. The Able-Entech SLA would require a slightly lower area of 2,400m² because of the higher efficiency produced from concentrating the sunlight and lower radiation induced degradation. The CIGS cells at 15% Beginning of Life efficiency and degraded for temperature, radiation, and packaging factor would require a 4700m² array that could be rolled out for deployment.

The two leading candidates for deploying these large solar arrays would be a “Square Rigger”²³ structure or a boom system similar that used on ISS for the Shuttle Radar Topography Mission²⁴ both developed by ABLE. The ISS boom was 60m, however similar lighter weight booms up to 100m are practical. AFRL PowerSail studies showed that 0.2kg/m² solar array structures were feasible. Table 3 shows the leading candidate solar technologies, efficiencies, area and width for a two-wing solar array deployed by a 60m boom. The Able-Entech SLA uses a “Square Rigger” deployment system made of composite tubes. This lightweight method of deployment can also be used with an ISS type solar panel using multi-junction or thin film cells.

An additional option would be to use the CIGS thin film cells at lower efficiency that require a larger deployed area. This could be accomplished by doubling the width of the wings mentioned above and by folding the array in the stowage fairing or by using a longer boom. Solar array structure systems such as inflatable structures, “Square Rigger”, pantograph, rolled, folded and other concepts also have viability for use on a large thin film solar array.

Table 3 Comparison of Advanced Solar Cell Technologies

	Beginning of Life Efficiency	Efficiency at Temp. and Radiation	Array Area for 600kW, m ²	Wing Width at 60m, m
CIGS Thin Film	16%	10.4%	4700	39.1
Multijunction GaAs	28.5%	19.5%	2600	22.1
Refractive Concentrator	~30%	22%	2400	20.7

VII. Plume Interactions

It is well known that Hall thrusters present special plume problems that are not encountered with ordinary chemical propulsion systems. Lockheed Martin has conducted several studies and IRAD efforts to develop the analysis tools that address the various concerns. A list of the commonly identified issues is as follows:

1. The ionized plume interference on spacecraft communications with ground stations
2. Spacecraft charging and electrostatic discharge
3. Erosion of surfaces (especially solar arrays) as a result of sputtering by the high energy ions
4. Contamination due to re-deposition of sputtered material
5. RF emissions from the plume interfering with payloads

The first step in analyzing the Hall thruster plume is to model the fluid dynamics. There are several techniques that can be used to analyze the fluid dynamics including sophisticated Direct Simulation Monte Carlo computer codes.²⁵ For this analysis the HET plume code is used,²⁶ which relies on both a Lagrangian primary beam algorithm and a Particle-in-Cell solver for computing ion production from charge-exchange reactions. The plume flow field can be computed self-consistently with the spacecraft geometry or, as is the case here, computed independently and then overlaid onto the geometry.

The effect of the ionized plume on communications with the ground is considered a minimal issue for an SEP cargo tug. Even though the ionized plume will be much larger than for any previous EP systems, a simple low gain S band omni patch antenna has been determined to be sufficient to cover lunar missions. Communications with an SEP tug is much simpler than GEO communications satellites where a complex beam pattern needs to be maintained.

Thruster plume interactions with surfaces are simulated using the Lockheed Martin Surface Effects Tool. This tool overlays a plume map onto a three dimensional spacecraft geometry and computes surface effects and interactions on impinged surfaces using a line of sight model. Erosion rates are computed using a rate model and a compiled sputter rate database.^{27,28} Contamination from re-deposition of sputtered material is subsequently computed using erosion quantities as input. Preliminary sputtering analyses have focused on calculating general sputter maps that can provide guidance for design of the space vehicle. One area of concern is the effect of the high energy plume on the very large solar arrays. A sputter map for one thruster operating at 150 kW is shown in Figure 15. The map indicates the possibility of significant erosion at all points in front of the thruster (plume angle less than 90°). More detailed analyses will be performed as the design matures.

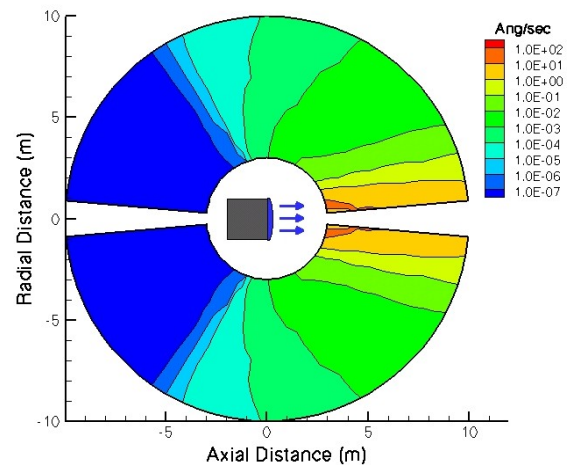


Figure 15 Erosion rate map for a single 150kW Hall thruster plume

VIII. Thermal System

At the electrical power level of multiple hundreds of kilowatts, which is required for a large SEP cargo tug, even small inefficiencies in power conversion and transmission can cause a large heating problem. The largest challenge is still in the PPU, even though conversion efficiencies are anticipated to eventually reach 96% for conventional PPUs. For the current 600kW vehicle under consideration this translates into 24kW of waste heat! This magnitude of energy rejection can present challenges in acquiring, transporting, and rejecting the thermal energy. Optimizing the thermal system is an important contribution towards an efficient and robust spacecraft design.

Typical spacecraft today range in power from several hundred watts to the multi-kilowatt range, for example the Boeing HS702 at 17 kW. The international space station (ISS) is the largest space vehicle ever built with electrical power in excess of 70kW. For most spacecraft the electrical power is distributed to

various avionics and is seldom concentrated into a small area; thus it is possible to mount the power dissipating electronics to a spacecraft structural panel and rely on that panel to radiate the heat to space. The key to using this simple technique is that the power must be spread over a large enough area. This requires that the component's power density (dissipation/footprint) be reasonably low. At higher levels the lateral conductivity of the panel must be augmented with added mass for heat conduction, typically in the form of metal or high-conductivity composite plates. Figure 16 shows a comparison between some typical conduction-cooled spacecraft components and the prototype Hall Effect PPU.

The PPU is clearly outside typical power densities. Normal thermal management techniques become impossible (or incredibly mass-intensive) at high power levels, and mass transport solutions must be employed. Spacecraft designers prefer to use embedded passive devices such as heat pipes, capillary pumped loops, or loop heat pipes because of their inherent reliability. These devices can be used to spread the heat over a larger portion of the spacecraft structure, but at some point the structure can no longer supply enough area to radiate all of the heat. At this point deployable radiators must be used adding the complication of providing flexible joints in the heat transport tubes. In theory there is almost no limit to how much heat such a passive system could handle since to increase capacity the designer can just add more heat pipes or loops and deployable radiators. As the deployed radiators increase in size the tubes increase in size and at some point this type of transport system becomes too heavy and impractical. At that point, the spacecraft designer must consider moving the heat transfer fluid with a mechanical pump.

The HS702 satellite uses a very complicated loop heat pipe radiator system to remove the 17 kW of heat while the ISS uses a mechanically pumped loop. The break point between passive and active system would seem to be somewhere above 17kw, however there is belief that the passive system for the HS702 was taking passive technology beyond its cost effective range. Although mechanical pumps are discouraged for spacecraft use due to the

potential for failure, there have been satellites other than the ISS which have used this type of heat transport system. For example the Mars Pathfinder lander used a mechanically pumped R-11 cooling loop to remove heat from the lander during the cruise phase. Since mechanically pumped cooling loops greatly simplify the thermal design one must weigh the advantages of simplicity against the perceived risk of pump failure.

The total amount of heat and the temperature at which the electronics must be controlled dictate the size of the radiators. For this study 24 kW must be rejected at approximately 100C depending on the cooling technique selected. With a perfect view to space the minimum radiator area needed is 19.7m². When imperfect view factors and other engineering considerations are taken into account the radiator size can easily grow by a factor of two. The size of these radiators coupled with packaging concerns make it difficult to conceive of a passive solution to the heat removal problem. If a mechanically pumped option is selected it widens the solution space to many engineering cooling options and advantages. In general there are three possible options for mechanically pumped loops; the first is a pumped single phase liquid such as was used on the Mars Pathfinder lander. Another option is a 2-phase pumped loop which uses a pump to move liquid to the heat source at which point the phase change energy of evaporation removes the heat and the vapor is condensed in the radiator, which has the advantage that the condensation maintains a high temperature on the radiator. Finally the cooling can be provided by a single phase gas loop which uses a blower to move the gas through the component in a manner very similar to terrestrial cooling schemes for high power electronics. Other cooling options available with mechanically pumped loops are pool boiling, immersion cooling, jet impingement cooling, droplet impingement, and enhanced convective surfaces (e.g. fins). The interface with the radiator can take various forms (See Figure 17) involving either heat pipes

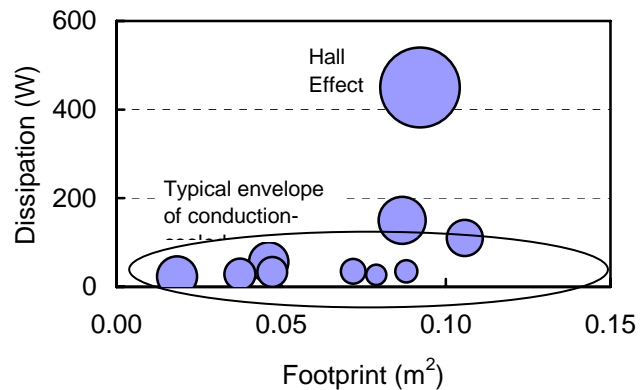


Figure 16 Power Density of the PPU vs. Flown Spacecraft Components

only, pumped transport with heat pipes onto the radiators, or pumped loops onto the radiator. All of the pumped-loop options shown could be either one or two-phase systems.

Each option has optimizations that must be examined involving working fluids and pressures, tube materials, number and size of the loops/pipes, flow speed and routing – all of these affect the ultimate performance of the heat rejection system. Despite the complexities of the solution space, ultimately the optimum design will be judged on familiar criteria: mass, packaging, and reliability. A preliminary radiator sizing model was employed to obtain sizings for different candidate systems, Table 4.

This model includes the mass required for the fluid loops, heat pipes, pumps, fluid, radiators, and micrometeoroid shielding. The two-phase systems have a clear advantage in area and mass, but further work must be done to ensure that the benefits of two-phase outweigh the increased complexities.

Mass savings are also possible by integrating the vehicle and component heat rejection designs. For instance, the fluid/gas loop could flow directly through a component and thus put the thermal interface directly at an electronic component. This eliminates the need for the component designer to conductively sink the card to the box baseplate, and for the spacecraft designer to sink the box to the spacecraft mounting surface. More significantly, the fluid loops acquire the waste heat at a higher temperature, allowing the heat rejection at the radiator to occur at a higher temperature, which reduces required radiator mass and size. This interface has significant benefits, but also requires significant work early in the spacecraft development cycle to ensure that the overall system and the component are designed in an integrated fashion.

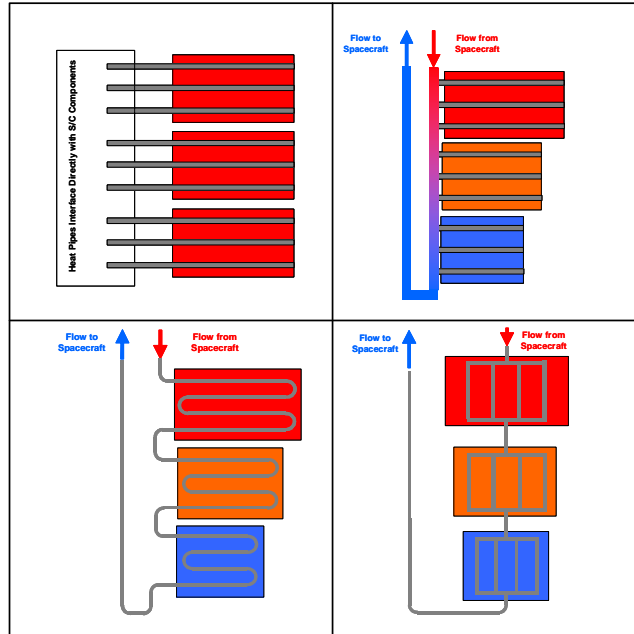


Figure 17 Candidate Radiator Designs

Table 4 Radiator Sizing for Several Heat Rejection Systems

	Rad. Area (m ²)	Mass (kg)	Inlet Temp(°C)
1-Φ Pump Through Radiator	54	63	100
2-Φ Pump Through Radiator	24	83	100
1-Φ Heat Pipe	52	112	100

IX. Propellant Storage

The propulsion system for the 600kW SEP vehicle consists not only of the main Hall effect thruster system, but also a standard hydrazine attitude control system, which is used for docking maneuvers as well as attitude control. Regardless of how the tug or cargo vehicles are configured, each cargo spacecraft will be required to bring up the propellant for its transfer to the Moon or Mars. This makes the xenon storage and feed system the single largest component of the cargo vessel. A conservative value of 30MT which was used as the design point for the storage and feed system trade study (the actual mass is closer to 24MT). Since xenon becomes liquid at a relatively high temperature compared to other more common gasses (-108°C at 0.1MPa) it was recognized that a cryogenic storage system might be a reasonable way to reduce weight and improve packaging.



Figure 18 PSI model 80442-1, 1.7MPa tank

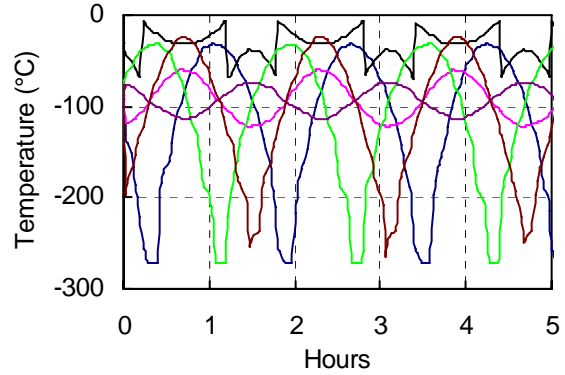


Figure 19 Orbital equivalent radiation temperatures

Standard oxidizer tanks are already designed to handle 1.7MPa (250psi) thus this was chosen as the most cost effective design pressure for a cryogenic system. Storing xenon at 1.7MPa has the added advantage of raising the boiling point to -35°C which is not a particularly difficult requirement to meet for most spacecraft thermal control subsystems. In order to get a realistic mass estimate for the cryogenic storage system it was decided to base the design on the largest off the shelf tanks available, thus the PSI model 80442-1 with a volume of 1.435m^3 shown in Figure 18 was selected. Including ullage, a total of 8 tanks are needed to store 30,000kg of liquid xenon at -35°C . Since liquid xenon is heavier than any oxidizer, a mass allocation for thicker walled tanks is made in order to handle launch loads. Next a simple orbital thermal analysis is done to determine the difficulty of maintaining temperatures less than -35°C . A simple six sided spacecraft model with an emissivity of 0.7 and a solar absorptivity of 0.1 (roughly equivalent to white paint) is analyzed for a 550km orbit. Figure 19 shows temperatures that would be expected from a structure of zero mass otherwise known as the equivalent radiation sink temperature. This simple analysis shows that except for the sun facing side a temperature of -35°C will be easily maintained if the propellant is sufficiently shielded from the rest of the relatively warm spacecraft and a reasonable radiation view factor of space is maintained.

To provide xenon at the required rate of 0.8g/s mass flow rate, heat must be added to boil the liquid xenon. Since the latent heat of vaporization for xenon is 99kJ/kg, an 80W electrical heater circuit is needed. The heater is turned on as necessary to maintain the proper tank pressure. It is recognized that there are ground handling issues such as water condensation while the tank is being filled or stored inside the payload faring. In order to minimize condensation, 1cm of low thermal conductivity foam is allocated for insulation. Ten layer multilayer radiation insulation (MLI) is used to provide the thermal radiation shield between the spacecraft and the tank system. The combined mass of the tanks, mounting hardware, plus insulation is 483 kg. It is noted that if a custom tank design is used such that only 4 or possibly 3 larger tanks are used, the mass of the cryogenic storage system is further reduced. It should also be noted that cryogenic storage systems are common technology for launch vehicles, launch vehicle upper stages, and spacecraft. Examples of each of these categories include: the Delta launch vehicle, the Atlas Centaur upper stage, and the Gravity Probe B spacecraft which stores liquid helium at 4K.

The comparable super critical (high pressure gas) tank design is based off of studies conducted for the Jupiter icy moon orbiter (JIMO). It has been found that the optimal storage pressure for xenon at 20°C is 12.1 MPa (1750 psia). The mass optimal tank necessary to store 30,000 kg of xenon is an 18.5 m^3 spherical titanium tank with composite over-wrap. This type of storage system has no need for special thermal insulation schemes thus the total mass of the system is simply the mass of the tank itself, 1050 kg. The conclusion of this study is that even with off the shelf tanks, the cryogenic storage system weighs less than half of the comparable high pressure system and is therefore clearly a superior system. The problems involved in maintaining the liquid xenon at a temperature of less than -35°C are minimal.

The remaining propulsion issue for this SEP vehicle is an attitude control system. In order to maintain attitude a simple monopropellant hydrazine propellant system with 133 N (30 lb) and 22 N (5 lb) thrusters is selected. Based on the mass and moments of inertia of the combined tug/cargo vehicle it is calculated

that 260 kg of propellant is needed. The mass of the tanks, pressure regulators, valves, lines and thrusters necessary for this subsystem is estimated to be 62 kg. This type of attitude control propulsion system is a low risk, well understood technology and will present no special integration problems or unexpected costs.

Xenon availability

A major issue for a solar electric propulsion cargo vehicle that employs xenon (Xe) as propellant is the concern over availability of large quantities of this noble gas. Global production of xenon in 2005 is estimated at roughly 40-50 MT per year; this compares with a production rate of around 23 MT per year in 1993²⁹. It is estimated that within 5 years, global production will increase to 70 MT per year naturally from increased demand from non-aerospace applications. The principal source of xenon is as a by-product from air liquification plants that separate out oxygen and have also installed xenon extraction columns. Principal uses of xenon are in the lighting industry for halogen bulbs and in the medical field to enhance x-ray images and as a safe general anesthetic.

A cargo tug that uses 20 MT of propellant would definitely affect the economics of xenon production internationally. However, this appears to be a very elastic market and as demand increases there is every reason to believe that global supply will rise in step. In order to obtain a cursory assessment of the global xenon production capability, six producers of xenon were contacted. It was the unanimous opinion of all companies contacted that an increase in production of 20 MT per year was quite feasible with a couple of years of planning to bring new and existing facilities on-line and a long-term contract to assure continued demand. The majority of Xe production is outside the U.S. with heavy producers being Russia, South Africa and China. It should also be noted that many companies presently have xenon production facilities sitting idle due to a previous overestimation of demand for the gas. Part of this overestimation is attributable to the Teledesic program of the late 1990's where it was speculated that an original constellation of 840 satellites was going to be built for broadband communications, with each satellite employing Hall thrusters that use xenon propellant. This constellation did not materialize and was suspended in October 2002.

Over the last 2 decades the cost of xenon has fluctuated between \$2-20 per liter and it currently sells for ~\$4-5 per liter. At \$5/liter, this translates into \$17M for propellant cost for a mission requiring 20 MT of Xe.

X. Discussion

The previous sections show that notable advancements are being made in all critical technologies needed to make an SEP cargo tug a reality. With continued development it is believed that a 30-50kW power level SEP tug could be available by 2011 and a high power, > 500kW version, could be built by ~2015. This system could save 10's of billions US dollars in reduced launch costs, as the nation embarks on the President's Vision for Space Exploration.

One of the major challenges of this effort was to determine if the SEP vehicle could be re-useable. The two main limiting factors are the solar array life due to radiation degradation and thruster life due to ion sputtering of the insulating channel walls. Both of these issues appear to be solvable for the desired 5 round trips of the tug. Although further investigation is clearly needed, analysis to date shows that several array technologies (the frontrunners being CIGS thin film and SLA) can meet the needed lifetime. The high power thrusters also appear to be able to meet life due to 1) the mechanical insulator actuation scheme being developed at NASA Glenn and 2) the high power naturally scales to a lower B field which implies that it should be easier to design the insulating channel with thicker walls.

The mass breakout for the OTV, given in Table 2, shows clearly that by far the largest dry mass subsystem of the tug is the solar arrays. Further improvements in this technology will have the largest impact on reducing system mass. Over the next 5 years it is estimated that solar array specific power will improve between ~50-80% for refractive concentrators and CIGS thin films. This specific power improvement corresponds to vehicle mass reductions of +1000kg. In less than 10 years it is anticipated that specific power will reach 500 W/kg which could translate into vehicle mass reduction of +1500kg from what is used in the mass model calculations for this paper. The solar arrays are also the major financial driver for a tug; it is possible that greater than a factor of 4 reduction in cost will accompany the improved specific power. Other technologies that help drive the mass of the tug down are: cryogenic propellant tank, direct drive power processing, light weight structures especially the thruster boom, compact thruster designs and an advanced thermal system.

Additional vehicle requirements that need to be evaluated further are: the build-ability of the overall system, the maximum allowable transit time of the cargo, reliability at the vehicle and sub-system level, and the overall cost of the system and its operation. Reliability is being initially considered in terms of redundancy of power processor components and thrusters. From an overall mission architecture, employing a reusable cargo tug translates to fewer launches which corresponds to higher overall mission reliability.

It can easily be seen that all versions of the SEP system deliver far more mass than the chemical system and in some cases more than doubling the delivered mass for the same number of launches. All of these configurations assumed a constant specific impulse for their hall thrusters. Given the effect of passing through the Van Allen belts on solar arrays and electronic devices on board the spacecraft and perhaps even the cargo itself, there is a potential benefit for lowering the specific impulse early on in the mission and decreasing the radiation exposure by reducing the time in this harsh environment. Additionally all of these concepts require the use of a large Shuttle-derived launch vehicle. Configurations that launch on smaller launch vehicles than the Shuttle-derived concept here may be capable of delivering the same mass as the chemical system without requiring the expenditures involved with building and launching such a massive launch vehicle.

Table 5 Comparison of Tug Economic Parameter between vehicle configurations

		Cryo Chemical	SEP Cargo Tugs		
		450 sec	2500 sec	3000 sec	3500 sec
Tug Economic Parameter (MT/\$M)		19.8	35.6	38.6	40.7

Economic Assessment

The ultimate driving force that will dictate whether an SEP cargo tug is developed is economics. The mission of the cargo tug is simply to transport cargo between points in space on an ‘as scheduled’ basis. This “semi-truck in-space” must accomplish its mission in the most cost effective manner possible. While an in-depth analysis of the cost of an SEP tug spacecraft is well beyond the scope of this effort, a first order assessment of the fiscal benefit of an SEP tug can be done. In order to lend some insight into the economics of this vehicle we have developed the following expression which we call the Tug Economic Parameter,

$$\text{Tug Economic Parameter} = \frac{\text{Total Cargo Delivered}}{\left(\text{Total Cost of Transport Vehicles}\right)\left(1 + \text{Interest Rate} * \text{Trip time}\right)}$$

This expression is a simple attempt to allow for a comparison between not only long trip time SEP and chemical, but also between the various Isp options for the SEP system. The Total Cargo Delivered is simply the amount of cargo delivered to the lunar surface over the life of the vehicle, which is assumed to be 5 round trips for all SEP tugs. Total Cost of Transport Vehicles includes the cost of the launch vehicle(s) plus tug cost. As a ROM for the cost of the vehicles, assume \$500M for both the cargo launch vehicle and the SEP cargo tug. Assume the chemical trans-lunar injection (TLI) stage is \$100M for the all chemical baseline. The expression, Interest rate*Trip time, is an attempt to penalize the SEP systems for their much longer transit length. This term is purely an inflationary cost term and does not include any operations cost.

The results, Table 5, show that for an annual interest rate of 10%, the SEP systems are taking about a 6% reduction in ‘benefit’ versus simply comparing the total cargo delivered for each tug. Basically, this reduces the SEP advantage by a minimal amount and this new technology still delivers roughly twice the benefit of a cryo chemical TLI/LOI stage. The annual interest rate needs to rise to >80% before the greater delivered payload for the higher Isp configurations no longer compensate for the longer required trip times. Interestingly, the interest rate needs to rise to >160% per year before the much greater cargo delivered benefits of an SEP cargo tug are nullified. This type of analysis still needs to be corrected for the fact that more vehicles are needed for longer transit time configurations if the vehicles are operated continuously.

XI. Conclusions

Mission analysis shows that an SEP cargo tug operating in the range of 3000 sec can deliver over twice the amount of payload to the lunar surface as compared to a cryogenic chemical system at 450 sec. Within 5-10 years, it is realistic to design an SEP tug that can operate for 5 round trips from LEO to LLO. The main life limiters are the solar array degradation and high power Hall thruster lifetimes. Fortunately, there are multiple solar array technologies presently under development that could lead to the needed specific power and radiation tolerance required for this mission. A potential scheme exists to lengthen the life of Hall thrusters to +30,000 hours of life, and possibly even 50,000 hours. The most significant mass savings for the SEP vehicle can be achieved by continuing to develop: advanced solar array technologies, cryogenic storage of the xenon propellant, direct drive power electronics, new compact thruster designs and light weight radiators. Although technology maturity is needed for most of the sub-systems that make up a high power SEP cargo tug, there appear to be no major technical hurdles that would prevent this vehicle from becoming a reality. The economic advantages of using solar electric propulsion for "semi-trucks in-space" appear to be exceptionally strong; this scheme of developing a SEP cargo tug has the potential to save 10's of billions of US dollars in reduced launch costs as part of the Vision for Space Exploration.

XII. Acknowledgements

This work was supported by NASA contracts NNC05CB08C, "600-kW High Thrust Hall thruster system (HESS)" monitored by Todd Peterson of NASA GRC and Nantel Suzuki of NASA HQ. Funding was also provided under contract NNC05CB09C, "Solar Electric Propulsion Direct Drive Demonstrator" also monitored by Todd Peterson of NASA GRC and Carlos Campos of NASA HQ. The authors strongly wish to express their gratitude to the following individuals for contributing to this paper: James Martin, Denise Kato of Lockheed Martin, Denver, Bill Meyer of Lockheed Martin Space Systems and Christian Carpenter of Aerojet - Redmond Operations.

References

- ¹ MSIS-E-90 density model, (<http://nssdc.gsfc.nasa.gov/space/model/models/msis.html>)
- ² Wertz, J. R., Larson, W. J., *Space Mission Analysis and Design, Third Edition*, Space Technology Library, 1999
- ³ CE&R CA-1 Midterm Report: Document 1, Attachment 1, Lockheed Martin Corporation, Point-of-Departure (POD) Lunar Exploration Requirements Document (LERD), Revision: Midterm Report Update, 10 June 2005
- ⁴ De Grys, K., et. Al., "4.5 kW Hall Thruster System Qualification Status," 41st Joint Propulsion Conference, AIAA-2005-3682, July 2005.
- ⁵ Manzella, D., et. Al., "Laboratory Model 50 kW Hall Thruster," 38th Joint Prop. Conf., AIAA-2002-3676, July 2002
- ⁶ Hofer, R. R., Peterson, P. Y., Gallimore, A. D., and Jankovsky, R. S., "A high specific impulse two-stage Hall thruster with plasma lens focusing," IEPC-01-36, 27th Intl. Electric Propulsion Conference, Pasadena, CA, Oct. 15-19, 2001.
- ⁷ Carpenter, C. and Patterson, M., "High-Current Hollow cathode Development," IEPC-01-274, October 2001.
- ⁸ Verhey, T.M., "28,000 Xenon Hollow Cathode Life Test Results", 25th International Electric Propulsion Conference, IEPC 97-168, August 1997.
- ⁹ Palluel, P., and Shroff, A.M., "Experimental Study of Impregnated-Cathode Behavior, Emission, and Life", Journal of Applied Physics. 51(5), May 1990.
- ¹⁰ Garner, C.E., et. Al., "A 5,730 Hr Cyclic Endurance Test of the SPT-100," 31st Joint Propulsion Conference, AIAA-1995-2667, July 1995.
- ¹¹ Hamley, J. A., et al. "Hall Thruster Direct Drive Demonstration." AIAA Paper 97-2787, 33rd Joint Propulsion Conference, Seattle, WA, 1997.
- ¹² Hoskins, W.A., et al., "Direct Drive Hall Thruster System Development," AIAA-2003-4726
- ¹³ Hoskins, W. A. et al. "Direct Drive Hall Thruster System Study." JHU-CPIA: 51st JANNAF Propulsion Meeting, Orlando, FL, Nov., 2002.
- ¹⁴ NASA Glenn Research Center, "Powering the Future NASA Glenn Contributions to the International Space Station (ISS) Electrical Power System," FS-2000-11-006-GRC, November, 2000.
- ¹⁵ Spectrolab, Inc., "28.3% Ultra Triple Junction (UTJ) Solar Cells," Retrieved from <http://www.spectrolab.com/DataSheets/TNJCell/utj3.pdf>, September 9, 2005.
- ¹⁶ National Renewable Energy Laboratory, "Cost Competitive Electricity from Photovoltaic Concentrators Called 'Imminent'," NREL NR-2405, July 13, 2005.
- ¹⁷ Roedern, B. von, et. al., "The Role of Polycrystalline Thin-Film PV Technologies for Achieving Mid-Term Market-Competitive PV Modules," 31st IEEE Photovoltaics Specialists Conf., Lake Buena Vista, FL, Jan. 3-7, 2005.
- ¹⁸ Alder, Aaron L., et.al., "AFRL PowerSail Structure for Large Solar Arrays," AIAA-2003-6356 Presented at Space 2003, Long Beach, CA, 23 - 25 September 2003.
- ¹⁹ T. Takamoto et al., "Future Development of InGaP/(In)GaAs Based Multijunction Solar Cells", Proceedings of the 31st IEEE-PVSC, Orlando, Florida, pp. 519-525 (2005).
- ²⁰ M. Kroon et al., "End-Of-Life Power Predictions of Cu(In,Ga)Se₂ Solar Cells", Proc 3rd WCPEC, Osaka, Japan, pp. 809-812 (2003).
- ²¹ Imaizumi, Mitsuru, et. al., "Results of Flight Demonstration of Terrestrial Solar Cells by MDS-1 in GTO," NASA/CP-2005-213431, 2005.
- ²² M.J. O'Neill et al., "Recent Technology Advances for the Stretched Lens Array (SLA), A Space Solar Array Offering State of the Art Performance at Low Cost and Ultra-Light Mass", Proceeding of the 31st IEEE-PVSC, Orlando, Florida, pp. 810-813 (2005).
- ²³ M.J.O'Neill, "ENTECH's Stretched Lens Array (SLA) for NASA's Moon/Mars Exploration Missions, Including Near-Term Terrestrial Spin-Offs", Intl. Conf. on Solar Concentrators for the Gen. of Electricity or Hydrogen, Scottsdale, Az, May 1-5, 2005.
- ²⁴ AEC-Able Corp. Datasheet, Feb. 2000. http://www.aec.able.com/srtm/srtm_spex.htm
- ²⁵ Boyd, I. D., "Numerical Simulation of Hall Thruster Plasma Plumes," 9th Spacecraft Charging Conference, Tsukuba, Japan, April, 2005.
- ²⁶ Katz, I., Dressler, R., Boyd, I., Kannenberg, K., Pollard, J., King, D., et al, "A Hall Effect Thruster Plume Model Including Large-Angle Elastic Scattering," AIAA 2001-3355, 37th AIAA/ASME/SAE/SAEE Joint Propulsion Conference, Salt Lake City, UT, July 9-11, 2001.
- ²⁷ Kannenberg, K., Khayms, V. Emgushov, E., Werthman, L., "Validation of Hall Thruster Plume Sputter Model," AIAA 2001-3986, 37th AIAA/ASME/SAE/SAEE Joint Propulsion Conference, Salt Lake City, UT, July 9-11, 2001.
- ²⁸ Hu, S., Anne, J., Khayms, V. Emgushov, E., Werthman, L., "Development of Sputter Database for Hall Thruster Plume Effects Evaluation," AIAA-2001-3356, 37th Joint Propulsion Conf., Salt Lake City, UT, July 9-11, 2001.
- ²⁹ Welle R.,P., "Xenon and Krypton Availability for Electric Propulsion: An Updated Assessment," AIAA 93-2401, 29th AIAA/ASME/SAE/SAEE Joint Propulsion Conference, Monterey, CA, June 28-30, 1993.